Published in final edited form as:
Cancer Res. 2014 October 1; 74(19): 5421–5434. doi:10.1158/0008-5472.CAN-14-0067.

Paclitaxel therapy promotes breast cancer metastasis in a TLR4-dependent manner

Lisa Volk-Draper[1,§], **Kelly Hall**[1,§], **Caitlin Griggs**[1], **Sandeep Rajput**[1], **Pascaline Kohio**[1], **David DeNardo**[2], and **Sophia Ran**[1,*]

[1]Southern Illinois University School of Medicine, Department of Medical Microbiology, Immunology and Cell Biology, Springfield, IL 62702-9678

[2]Washington University School of Medicine, Department of Medicine, Oncology Division, St. Louis, MO 63110

Abstract

Emerging evidence suggests that cytotoxic therapy may actually promote drug resistance and metastasis while inhibiting the growth of primary tumors. Work in preclinical models of breast cancer have shown that acquired chemoresistance to the widely used drug paclitaxel (PXL) can be mediated by activation of the Toll-like receptor TLR4 in cancer cells. In this study, we determined the pro-metastatic effects of tumor-expressed TLR4 and PXL therapy and we investigated the mechanisms mediating these effects. While PXL treatment was largely efficacious in inhibiting TLR4-negative tumors, it significantly increased the incidence and burden of pulmonary and lymphatic metastasis by TLR4-positive tumors. TLR4 activation by PXL strongly increased the expression of inflammatory mediators, not only locally in the primary tumor microenvironment but also systemically in the blood, lymph nodes, spleen, bone marrow and lungs. These pro-inflammatory changes promoted the outgrowth of Ly6C+ and Ly6G+ myeloid progenitor cells and their mobilization to tumors, where they increased blood vessel formation but not invasion of these vessels. In contrast, PXL-mediated activation of TLR4-positive tumors induced de novo generation of deep intratumoral lymphatic vessels that were highly permissive to invasion by malignant cells. These results suggest that PXL therapy of patients with TLR4-expressing tumors may activate systemic inflammatory circuits that promote angiogenesis, lymphangiogenesis and metastasis, both at local sites and premetastatic niches where invasion occurs in distal organs. Taken together, our findings suggest that efforts to target TLR4 on tumor cells may simultaneously quell local and systemic inflammatory pathways that promote malignant progression, with implications for how to prevent tumor recurrence and the establishment of metastatic lesions, either during chemotherapy or after it is completed.

Keywords

Paclitaxel; chemoresistance; TLR4; breast cancer; lymphatic metastasis

[*]Corresponding Author: Sophia Ran, Southern Illinois University School of Medicine, Department of Medical Microbiology, Immunology, and Cell Biology, Springfield, IL 62702-9678. Phone: (217) 545-7026; Fax: (217) 545-3227; sran@siumed.edu.
[§]These authors contributed equally to this work

Disclosure of Conflict of Interests: The authors disclose no potential conflicts of interest

INTRODUCTION

Paclitaxel (PXL) is a widely-used drug for breast cancer (BC) treatment with an overall response rate of 25% (1). The advanced PXL formulation as albumin-embedded nanoparticles (nab-PXL) increased the initial response rate to 42% (2); however, resistance occurs frequently and the evasion mechanisms remain unclear. Tumor recurrence occurs in 30% of node-negative patients, and up to 70% in node-positive BC patients (3). Only 23% of relapsed patients survive five years after diagnosis mainly due to metastasis to lymph nodes (LNs) and distant organs (4). Several recent studies suggest that PXL (5,6) both kills and activates tumor cells thereby increasing chemoresistance and metastasis. The goal of this study was to delineate the mechanisms underlying relapse-associated metastasis possibly driven by PXL therapy.

Tumor resistance to PXL is currently thought to be due to either overexpression of transporters that decrease intracellular drug concentrations or preexisting mutations preventing drug binding to tubulin (7). We recently identified a novel mechanism of chemoresistance to PXL relating to its activation of Toll-like Receptor-4 (TLR4) (8). TLR4 is expressed mainly in the antigen-presenting cells that respond to lipopolysaccharide (LPS), a component of bacterial membrane (9). Macrophages activated by LPS•TLR4 pathway acquire the capacities to quickly migrate to an infected site, protect themselves from pathogen toxicity, destroy invaders, and restore homeostasis to the injured tissue (9). While these TLR4-dependent macrophage functions are essential for body defense, overexpression of TLR4 in tumor cells has deleterious consequences due to acquisition of a migratory, toxicity-resistant and “wound healing”-like phenotype. Albeit not universally recognized, TLR4 is often expressed and activated in human cancers by the products of injured and dead cells typically present in the tumor environment and particularly increased after chemotherapy (10). In addition to endogenous TLR4 ligands, this receptor is also activated by PXL (11) suggesting that this type of therapy can enhance recurrence and metastasis in TLR4-positive tumors (5,8).

This notion is strongly supported by multiple clinical studies showing that TLR4 expression correlates with tumor de-differentiation (12), higher clinical stage (13), faster recurrence rates (14,15), infiltration by inflammatory myeloid cells (14), higher incidence of venous invasion (16) as well as lymphatic and distant (14,16,17) metastasis. Tumor expression of TLR4 also correlates with shorter relapse-free and overall survival in breast (14), colorectal (17), and pancreatic (16) human cancers. Moreover, mechanistic studies in multiple cancer models showed that LPS activation of tumor-expressed TLR4 increases expression of angiogenic and inflammatory factors (5,18), immune evasion (18), cell survival (19), invasiveness (20), and metastatic spread (15). Studies in human ovarian cancer models were first to show that both LPS and PXL cause significant inflammation and protection from cell death mediated by an intracellular adaptor of TLR4, MyD88 (5,21). The latter is highly upregulated in clinical ovarian cancer and strongly correlates with decreased patient survival (22,23). Knockdown of TLR4 restored sensitivity to PXL (5,21) and conferred a less metastatic phenotype (24) compared with isogenic TLR4-rich tumors.

In line with this evidence, we recently reported that TLR4 overexpression in a negative BC line HCC1806 substantially increased inflammation and chemoresistance to PXL therapy (8). Consistently, suppression of TLR4 expression in a positive MDA-MB-231 line significantly improved response to PXL resulting in a 6-fold increase in the number of tumor-free mice (8). Here, we aimed to delineate the mechanisms by which PXL in conjunction with TLR4 impairs tumor response to PXL therapy. Among various functional consequences of TLR4 activation, we considered that LPS activated macrophages rebuild vascular networks through recruitment of bone marrow (BM) progenitors (25). Extrapolating from that, we postulated that PXL-driven TLR4 activation in tumor cells may recapitulate this phenotype leading to tumor recruitment of pro-vascular progenitors, increased vessel formation and tumor spread.

To test this hypothesis, we analyzed the effects of PXL therapy on inflammation, tumor vascularization, growth, and metastasis in both syngeneic mouse and human BC models with differential expression of TLR4. We found that PXL increases local and systemic inflammation concomitant with expansion of tumor vascular networks, increased lymphatic metastasis and significantly worse outcome in TLR4-positive as compared with negative or untreated tumors. These findings suggest that blocking the TLR4 pathway may restore sensitivity to PXL therapy and significantly improve cancer patient survival.

MATERIALS AND METHODS

Materials

TRI-reagent and protease inhibitors were purchased from Sigma-Aldrich (St. Louis, MO). Dulbecco's modified Eagle's medium (DMEM) and supplements were from Lonza (Switzerland). Paclitaxel albumin-bound nanoparticles (nab-PXL) were obtained from a local hospital pharmacy.

Antibodies

Primary antibodies were: rat anti-mouse CD11b, Ly6C, Ly6G and MECA-32 (BioXCell, NH); rabbit anti-mouse Lyve-1 and Prox1 (Angiobio, CA); mouse anti-human HLA (ATCC, VA); and PE-rabbit anti-mouse Ly6C (BD Bioscience, NJ). Anti-specie-specific secondary antibodies conjugated to 488, 549 and 650 dyes were from Jackson ImmunoResearch Laboratories (West Grove, PA).

Cell lines

Luciferase-tagged human MDA-MB-231 and HCC1806 cell lines were stably modified to either suppress or upregulate TLR4 expression as described previously (8). Modified lines and the corresponding controls were designated as 231^{TLR4+} and 231^{TLR4-} (derived from MDA-MB-231) or 1806^{TLR4-} and 1806^{TLR4+} (HCC1806). MMTV-PyMT mouse BC line was generated in Dr. DeNardo's lab. Other mouse BC lines were obtained from ATCC. All lines were cultured in 5% DMEM with standard additives at 37°C in 10% CO_2. All human lines were authenticated by ATCC in 2013 and tested for mycoplasma using a kit from R&D Systems (Minneapolis, MN).

Generation of dominant-negative (DN) TLR4 and MyD88 cell lines

MDA-MB-231 cells were stably transfected with DN-TLR4 and DN-MyD88 using pZero-hTLR4a and pdn-MyD88, respectively. Control lines were similarly generated using corresponding empty plasmids (pZero-MCS and pDeNy-MCS) from InvivoGen (San Diego, CA).

Animal studies

Tumor growth was monitored as described (8,26). Briefly, 4×10^6 (human) or 0.5×10^6 (mouse) cells suspended in 50% Matrigel were implanted orthotopically into 4–6 week-old female SCID, C57BL/6 or BALB/c mice (Taconic, NY) followed by measurements 3 times a week using digital calipers. When tumors reached 150 or 500mm^3 mice were treated with 10–30mg/kg nab-PXL for 2 cycles of five consecutive days with one week rest between the cycles. Tumors, serum, and organs were collected when tumors reached 1800mm^3. Animal care was in accordance with institutional guidelines.

Determination of metastatic burden

Tissues were homogenized in ice-cold lysis buffer (Promega, WI) containing protease inhibitors. Luciferase substrate (50μl) was mixed with lysates (10μl) followed by luminescence detection using a luminometer (Berthold, Germany). Extracts with luciferase activity of 1,000RLU/s above background were considered positive for metastasis. Data are expressed as the mean RLU/s ±SEM from duplicate readings normalized per mg of total protein determined by Bradford assay.

RT-qPCR

RNA was extracted from tumors, lymph nodes, and lungs by TRI-reagent and reverse transcribed using RevertAid cDNA synthesis kit (Fermentas, Canada). Primers were designed based on CDS of targets found in NCBI database. All primer sequences are listed in supplementary Table S1, and were validated to be human- or mouse-specific. Transcripts were analyzed using GoTaq Green Master Mix (Promega) and MasterCycle *realplex* PCR machine (Eppendorf, NY). Data were normalized to β-actin and relative changes in mRNA expression were determined using the ΔΔCt method.

Measurement of cytokine concentration by ELISA

Serum and tumor lysates were collected from tumor bearing mice treated with sterile endotoxin-free saline or 10–30mg/kg of nab-PXL and sacrificed on day 6 or 14 post treatment. IL-6, IL-8, CCL2, and IL1β concentrations were measured by ELISA according to manufacturer's instructions (Peprotech, NJ). All experiments were performed in duplicate and reproduced twice. Results are presented as mean pg ±SD normalized per mg of protein.

Measurement of spleen weight

Spleens were harvested from untreated or nab-PXL treated mice bearing 1806^{TLR4-} or 1806^{TLR4+} tumors. Results are presented as the mean spleen weight ±SD for each group (n= 3–5 mice).

Flow cytometry

Flow cytometry was performed on whole BM, spleen-derived mononuclear cells, and $CD11b^+$ cells from tumors. BM was collected by flushing the bones with 2% FBS and 1mM EDTA in PBS. Spleen mononuclear cells were obtained from a single-cell suspension followed by a Ficoll-Paque gradient. Tumor-associated $CD11b^+$ cells were isolated using rat anti-CD11b magnetic beads (MiltenyiBiotec, CA) from digested tumors by 225U/ml collagenase type III and 100U/ml hyaluronidase (Sigma-Aldrich, MO). After blocking Fc, cells were incubated with anti-CD11b, Ly6C, and Ly6G for 30min on ice followed by incubation with secondary 488- and 650-conjugated anti-rat antibodies. Expression was analyzed using AccuriC6 flow cytometer (BD Accuri Cytometers, MI) and FlowJo software (Ashland, OR). Results are expressed as mean % of marker expression per group (n=5) ±SEM.

Immunohistochemical analysis of blood vessels, lymphatic vessels, and macrophages

Acetone-fixed 8-μm-thick frozen tumor sections were rehydrated in PBS with 0.1% Tween20 (PBST) prior to incubation with anti-mouse CD11b, Ly6C, Ly6G, MECA-32, Lyve-1 diluted 1:100, or w6/32 hybridoma supernatant used undiluted. All antibodies were incubated with tissues for 1hour at 37°C with 10min wash in PBST between incubations. After the last wash, slides were mounted in VectaShield medium containing 4, 6′-diamidino-2-phenylindole (DAPI) nuclear stain (Vector Labs, UK). Images were acquired on an Olympus BX41 microscope equipped with a DP70 digital camera and DP Controller software (Olympus, PA).

Quantification of stained cells

Images of 6 random fields were taken at 200x magnification from sections stained with anti-CD11b, -Ly6C and -Ly6G. Images were analyzed by ImageJ software to determine fluorescent intensity for individual pixels. The amount of pixels acquired from positive staining was divided by the total pixels per field yielding the area-normalized % of positive staining for each specific marker. The results are presented as mean percent of marker expression per field ±SD (3 mice per group).

Quantification of blood and lymphatic vessel densities

BVD and LVD were determined from four images per slide captured at 200x magnification in tumor sections stained with either anti-MECA-32 or anti-Lyve-1 antibodies (3 mice per group). Vascular structures were enumerated using ImageJ. BVD is presented as the mean number of vessels per field ± SEM while LVD is the mean number of $Lyve\text{-}1^+$ structures normalized per mm^2 of the section area ± SEM.

Quantification of vascular invasion

Tumor sections were double-stained with anti-human HLA and anti-mouse MECA-32 or Lyve-1 antibodies as described above. Blood and lymphatic vessels with open lumens were identified and enumerated in each section. The percentage of open-lumen vessels invaded by tumor cells was normalized per section area. Results are presented as the mean % of invaded

vessels from total open-lumen blood or lymphatic structures normalized per section area ±SD.

Statistical analysis

Statistical analyses were performed using GraphPad Prism software. Results are expressed as mean ±SEM or ±SD. Statistical significance for continuous variables and categorical covariants was determined by Student's paired *t*-test and Chi-square test, respectively. Metastatic burden and incidence was assessed by Mann-Whitney and Fisher-exact test, respectively. P-values ≤0.05 were considered significant.

RESULTS

TLR4 expression in BC cells dictates the response to PXL therapy and metastatic spread

We previously showed that PXL elicits strong inflammatory responses and promotes tumor growth in TLR4-positive MDA-MB-231 and HCC1806 models, but not in isogenic controls with low or no TLR4 expression (8). Here, we confirmed that PXL effect is largely mediated via TLR4 because MDA-MB-231 cells overexpressing dominant-negative (DN) TLR4 or its intracellular adaptor MyD88 had substantially lower responses to PXL than vector-transfected controls (suppl. Fig. S1). We also confirmed that the pro-inflammatory response is not restricted to nab-PXL as both Taxol (8) and docetaxel (suppl. Fig. S2) similarly activate TLR4-positive tumor cells.

While our first study (8) focused on the effects of TLR4 and PXL therapy on growth and recurrence of primary tumors, here we used the same BC models to analyze the effects on metastasis. LN and lung metastasis was analyzed in mice with orthotopically implanted 231^{TLR4+}, 231^{TLR4-}, 1806^{TLR4-} or 1806^{TLR4+} tumors that were either treated with nab-PXL (10mg/kg for 10 days) or left untreated. Consistent with prior results (8), TLR4 expression in both BC models was associated with 2–3 fold accelerated tumor growth and a higher resistance to nab-PXL compared with controls (Figs. 1A, 1B). Additionally, both TLR4 and PXL strongly affected the incidence and metastatic burden. For instance, nab-PXL treatment decreased the burden but failed to reduce 100% metastatic incidence in mice with TLR4-expressing 231^{TLR4+} tumors. In contrast, the same treatment of an isogenic model with 90% depleted TLR4 drastically decreased both burden and incidence of LN and lung metastases (Figs. 1C, 1E, 1G and supplementary Table S2).

The pro-metastatic role of TLR4 amplified by chemotherapy was even more pronounced in the HCC1806 model in which nearly all treated mice (90%) with $TLR4^+$ tumors were positive for LN and pulmonary metastases compared with less than half of the mice bearing isogenic negative tumors (Fig. 1D). Importantly, only in 1806^{TLR4+} tumors, nab-PXL therapy increased the burden of LN metastasis by 245-fold compared with untreated controls (P-value=0.008, suppl. Table S2). Chemotherapy also increased pulmonary metastasis by 12-fold in $TLR4^+$ and 5-fold in negative tumors (Figs. 1F, 1H) suggesting that some oncogenic effects of PXL are TLR4-independent. Cumulatively, these results show that PXL activation of TLR4 in tumor cells promotes tumor growth and metastasis, and that PXL therapy may result in a strikingly different outcome depending on expression of TLR4.

PXL in concert with TLR4 promotes local inflammation in primary human xenografts

We next delineated the mechanisms by which TLR4 and PXL advance metastatic spread. TLR4 is the major inducer of inflammation in injured or pathogen-attacked tissues (27). We therefore hypothesized that nab-PXL activation of TLR4 promotes metastasis by increasing tumor inflammation. To test this hypothesis we compared the cytokine expression in untreated and nab-PXL treated TLR4-negative and -positive tumors isolated 6 days post-treatment. Tissues were analyzed by RT-qPCR for expression of 15 inflammatory cytokines typically upregulated by TLR4 pathway (8). Chemo-treatment of mice with TLR4-negative tumors increased only a third of the examined cytokines by 2–3 fold (Fig. 2A). In contrast, treatment of mice with TLR4-positive tumors elevated 73.3% of cytokines up to ~12-fold (Fig. 2B). This result demonstrates that nab-PXL induces a significantly stronger inflammatory response in $TLR4^+$ tumors than those lacking this receptor.

Remarkably, the mere expression of TLR4 in malignant cells caused significant pro-inflammatory changes in the tumor environment as evident by highly increased levels of IL-6 (92.6-fold, IL-10 (39.3-fold) and IL-1β (16.4-fold) as compared with TLR4-negative controls (Fig. 2C). This pro-inflammatory pattern was intensified by nab-PXL that further increased IL-6 and IL-1β by, respectively, 276-fold and 57-fold (Fig. 2D). Protein analysis by ELISA confirmed TLR4-dependent alterations in the inflammatory profiles induced by PXL (Figs. 2E–H). IL-6 protein was undetectable in TLR4-negative tumors, but its expression increased to 56 pg/mg in TLR4-positive ones and amplified by 470% by nab-PXL treatment (Fig. 2E). The changes in IL-8 expression mirrored this pattern with barely detectable protein in TLR4-negative tumors and >10-fold upregulation in the TLR4-positive ones following nab-PXL treatment (Fig. 2G). The differences between TLR4-negative and -positive tumors were maintained throughout the experiment as evident by highly expressed cytokines in the TLR4-positive groups 2 weeks after treatment (Figs. 2F, 2H). Taken together, these data indicate that PXL activation of TLR4 substantially upregulates a wide range of cytokines causing a sustained inflammatory state in the local tumor environment which likely contributes to development of metastasis.

PXL•TLR4 pathway increases inflammation and metastasis in syngeneic mouse models

We then determined whether similar effects occur in syngeneic mouse models having intact adaptive immunity. We first screened several BC mouse lines *in vitro* to identify lines positive for TLR4 and responsive to PXL. We found that all examined lines (MMTV-PyMT, 4T1, 66.3 and EMT6) highly express TLR4 as well as all major regulatory components of the TLR4 pathway (Figs. 3A and 3B). MMTV-PyMT and EMT6 models were selected for *in vivo* analysis. Both models showed similar increases in intratumoral inflammatory cytokines after PXL treatment (Figs. 3C, 3D) to those observed in human xenografts (Fig. 2). EMT6 tumors were also analyzed for the effects on tumor growth and metastasis. Similarly to results in human BC models, nab-PXL therapy suppressed the growth of primary tumors (Fig. 3E), but significantly elevated metastasis (Fig. 3F). These data suggest that PXL and TLR4 cause similar pro-oncogenic and inflammatory changes in both human xenograft and syngeneic mouse models.

PXL activation of tumor TLR4 also enhances systemic inflammation

LPS-mediated activation of TLR4 increases systemic inflammation to alert distant organs of pathogen invasion and recruit immune cells first for body defense and, subsequently, for tissue healing (28). We postulated that PXL activation of TLR4 in malignant cells mimics this pattern by increasing inflammatory cytokines in the blood and distant organs responsive to TLR4 systemic signals. To test this hypothesis, we determined the pro-inflammatory effects of TLR4 and nab-PXL on blood-circulating IL-6 and IL-8 and multiple cytokines in the main metastatic organs, i.e., LNs and lungs.

The results showed that PXL activation of TLR4 significantly changed the inflammatory milieu in both blood and distant organs. Following treatment, levels of blood-circulating IL-6 and IL-8 proteins were highly increased in TLR4-positive (but not negative) group from undetectable to, correspondingly, 80 and 330pg/ml (Figs. 4A–4D). These cytokines were derived from human tumor cells because ELISA was performed using human-specific antibodies.

We also analyzed the expression of inflammatory cytokines in LNs and lungs from untreated and nab-PXL treated mice with TLR4-positive or -negative tumors. This analysis was performed with specie-specific primers validated on mouse and human universal cDNA (Suppl. Table S1). Transcripts of human cytokines were undetectable in distant organs; however, all groups showed changes in mouse host cytokines that closely followed transcriptional alterations in primary tumors (Fig. 2). In mice with TLR4-negative tumors, therapy caused a modest 2–3 fold increase in isolated LN cytokines. In contrast, in mice with $TLR4^{+}$ tumors, 40% of the examined LN cytokines increased by 4–8 fold. Similarly, nab-PXL did not affect lung cytokines in mice with TLR4-negative tumors, but increased many cytokines 3–4 fold in mice with $TLR4^{+}$ tumors (Figs. 4G–H). CCL20, IL-4, IL-6 and IL-10 were amongst the highest upregulated in both LNs and lungs. Collectively, these data indicate that PXL activation of TLR4 at the primary tumor causes profound systemic changes in expression of inflammatory mediators in the blood, LNs and lungs, the two main organs that permit growth of metastatic BC cells.

TLR4-mediated systemic inflammation increases generation of myeloid progenitor cells in bone marrow (BM) and spleen

TLR4-induced cytokines (e.g., IL-1β, IL-10, IL-6) have been reported to induce generation of myeloid progenitors that promote metastasis (29). Since these cytokines were highly upregulated both locally and systemically by TLR4•PXL axis, we hypothesized that their production enhances generation of myeloid progenitor cells in the distant organs such as BM and spleen. Indeed, the average spleen weight in mice with $TLR4^{+}$ tumors was 300% larger than that in mice bearing tumors lacking TLR4 (Figs. 5A–B). Moreover, nab-PXL treatment doubled spleen weight in mice with 1806^{TLR4+} tumors making them 6-fold larger than in untreated controls. Notably, spleens of mice with TLR4-negative tumors were unchanged by chemotherapy (Figs. 5A–B).

We next determined whether the increase in spleen size is due to generation of myeloid progenitors rather than edema or elevated hematopoiesis. Spleen and BM-derived cells were

double-stained for CD11b and the markers of immature myeloid cells, Ly6C and Ly6G, followed by FACS analysis and calculation of marker-positive fractions. FACS analysis revealed two major subsets labeled as Set 1 and Set 2 (suppl. Fig. S3). The most conspicuous difference was detected in Set 2 that consisted of ~5% of double-stained $CD11b^+/Ly6C^+$ cells in BM of mice with TLR4-negative tumors, but nearly 99% in both BM and spleen in mice with $TLR4^+$ tumors (Figs. 5C–D). Nab-PXL also increased a $Ly6G^+$ subpopulation from ~8% to 38% of $CD11b^+$ cells (4.75-fold) in both BM and spleen (Figs. 5E–F). Collectively, these data suggest that PXL therapy, particularly in the context of $TLR4^+$ tumors, significantly increases generation of immature myeloid cells that may promote metastasis (29).

Tumor-recruited myeloid progenitors increase blood vascular density (BVD) but not invasion of blood vessels

We next examined the effects of activated TLR4•PXL axis on tumor recruitment of myeloid progenitors and their contribution to vascular formation. Mice with TLR4-positive and -negative tumors were treated for 6 days with nab-PXL or left untreated. The excised tumors were stained with anti-CD11b, Ly6C, and Ly6G antibodies followed by quantification of pixels per field (Fig. 6). As compared with controls, a higher number of $CD11b^+$ cells were detected in TLR4-positive tumors after nab-PXL treatment than in those lacking TLR4 (3.3-fold *vs.* 1.9-fold, respectively; Figs. 6A, 6B). $Ly6C^+$ and $Ly6G^+$ cell recruitment showed a similar pattern. After chemotherapy, 1806^{TLR4+} tumors recruited ~7-fold more $Ly6C^+$ cells than TLR4-negative tumors (Figs. 6A, 6C). Following this trend, PXL treatment of 1806^{TLR4+} tumors mobilized ~3-fold more $Ly6G^+$ cells than negative tumors following identical therapy (Figs. 6B, 6C, 6D; statistically significant differences are identified by asterisks).

Because $Ly6C^+$ and $Ly6G^+$ cells have been reported to promote tumor blood vasculature (30), we determined the effects of TLR4 and PXL therapy on formation of blood vessels. We found that BVD was significantly increased by 2.5-fold (P-value <0.001) in treated mice with 1806^{TLR4+}, but not in other experimental groups (Figs. 6E, 6F). The role of immature myeloid cells in chemotherapy-driven vascular formation was also supported by treatment with anti-$CD11b^+$ antibody which significantly reduced intratumoral densities of both $CD11b^+$ monocytes and blood vessels (suppl. Fig. S4). We next determined whether increased BVD corresponded to enhanced tumor cell invasion of these vessels. Tumors were double-stained with w6/32 (anti-human HLA) and MECA-32 (anti-mouse BV marker) antibodies followed by quantifying the percent of tumor-invaded vessels of total open-lumen $MECA\text{-}32^+$ structures. Following nab-PXL treatment, TLR4-positive tumors displayed slightly higher density of invaded blood vessels (~3% as compared with 0.2% in TLR4-negative group); however, this difference was not statistically significant (Fig. 6G). This suggested that although TLR4•PXL-recruited $Ly6C^+$ and $Ly6G^+$ myeloid cells enhanced formation of new blood vessels they had no effect on tumor invasion of these vessels.

Activation of TLR4•PXL axis creates *de novo* intratumoral lymphatics and promotes their invasion

Since increased metastasis could not be explained by enhanced invasion of blood vessels, we hypothesized that the pro-metastatic effect of TLR4•PXL axis might be mediated through increased tumor cell access to lymphatics. To test this hypothesis, we re-stained tumors shown in Fig. 6 for lymphatic-specific markers. As previously reported (31), native HCC1806 tumors lack intratumoral lymphatics although they are rich in peritumoral Lyve-1^+ structures as shown in Fig. 7A. This pattern did not change in the absence of TLR4 or omission of PXL therapy. In sharp contrast, all treated mice with 1806^{TLR4+} tumors display extensive network of intratumoral lymphatics as shown in the last panel of Fig. 7A. The mean LVD in this group was 5.0±0.7 Lyve-1^+ vessels/mm^2 which was ~25 fold higher than in any other group (Fig. 7D). These *de novo* created vessels, residing as deep as 792μm from the tumor margin, displayed clear lymphatic phenotype as shown by mutually exclusive staining pattern with a blood vascular-specific marker, MECA-32 (Fig. 7B), and confirmed by another lymphatic-specific marker, Prox1 (Fig. 7C). Importantly, the new intratumoral lymphatics were highly permissive for tumor cell invasion as demonstrated by the drastically increased fraction of occluded Lyve-1^+ vessels that increased from zero in TLR4-negative tumors to 42% in TLR4-positive tumors treated by nab-PXL (Fig. 7D). In comparison, only 8% of lymphatic vessels were invaded in 1806^{TLR4+} tumors without treatment. Noteworthy that albeit TLR4-negative tumors were surrounded by Lyve-1^+ peritumoral vessels (Fig. 7A), most of them showed no signs of invasion (Fig. 7F). In sharp contrast, the majority of both peritumoral and intratumoral Lyve-1^+ vessels in TLR4-positive tumors after chemotherapy were invaded by malignant cells (Fig. 7G). These findings demonstrate a paramount role of tumor-expressed TLR4 in PXL chemotherapy-driven lymphatic metastasis.

DISCUSSION

Emerging evidence derived from recent clinical and experimental studies highlights the dark side of chemotherapy, namely, its alarming association with metastatic relapse after treatment. In particular, clinical studies showed a link between the widely-used drug paclitaxel (PXL) and substantial increase in lymphatic metastasis (32), tumor recruitment of pro-metastatic myeloid cells (32), circulating inflammatory cytokines (33), intratumoral COX-2 (34), and resistance to cytotoxic therapy (35). PXL was also shown to significantly promote metastasis in a transgenic BC model MMTV-PyMT (32), orthotopic human breast (26) and ovarian (36) xenografts as well as syngeneic models of melanoma and colon cancer (6). Mechanistically, the pro-metastatic effects of PXL can be attributed to its ability to induce NF-κB-dependent inflammatory, angiogenic and pro-survival factors that either directly enhance tumor aggressiveness (37) or mobilize BM myeloid cells that promote tumor spread via paracrine loops (32). We recently proposed that pro-metastatic effects of PXL are mediated by tumor-expressed TLR4 (8). Macrophage-expressed TLR4 is a naturally designed pathway that propagates inflammatory local and systemic circuits that expand pools of myeloid progenitors and recruits them to sites of inflammation to repair injured vasculature. We previously showed that $TLR4^+$ tumors vigorously react to PXL therapy by upregulating inflammatory mediators that create a favorable environment for

expansion of primary tumors (8). Here, we used mouse and human BC models with differential expression of TLR4 to analyze its role in promoting vasculature that subsequently increases locoregional and distant metastasis following the PXL therapy.

This analysis showed that both TLR4 and PXL play paramount roles in determining the magnitude of metastatic spread. Even in the absence of treatment, TLR4 expression in tumor cells caused multi-fold increases in both inflammatory cytokines and metastasis compared with tumors lacking this receptor (Figs. 1, 2). This drug-independent activation of TLR4 might be mediated by endogenous ligands overexpressed in BC such as hyaluronan (38), and S100A8/A9 (39). We also observed TLR4-independent effects of PXL which was evident by moderately enhanced inflammation and metastasis in tumor models lacking this receptor (Fig. 2). This effect might be mediated by TLR2 receptor (40) or by sensory receptors such as RAGE (25) and TREM-1 (41), all of which are known to be activated by the products of dead cells generated by chemotherapy. This scenario may explain pro-metastatic effects of chemotherapeutics other than PXL including cyclophosphamide (42), gemcitabine (43) and cisplatin (6,43). However, combination of PXL and TLR4+ tumors significantly increased the magnitude of the effect resulting in a 500% increase in incidence of LN and pulmonary metastasis and up to 245-fold elevated nodal burden (Suppl. Table S2). This was concomitant with ~300-fold increase in intratumoral inflammatory mediators (Fig. 2D) implicating the inflammatory consequence of the activated PXL•TLR4 pathway as the primary cause of increased metastasis.

Notably, PXL-dependent activation of TLR4 increased inflammation not only in the local tumor environment, but also in the blood, LNs, BM, spleen, and lungs (Figs. 4 and 5). This observation is not surprising given the natural function of macrophage-expressed TLR4 to systemically alert responsive organs for the presence of pathogens urging them to generate hematopoietic and endothelial progenitors. Under normal circumstances, these progenitors are recruited to the pathogen-invaded site to replenish the pool of immune cells, clear debris, and restore tissue homeostasis including the repair of vasculature. Analogously, in mice with $TLR4^+$ tumors PXL induced strong responses in BM and spleen resulting in ~20-fold increase in $CD11b^+/Ly6C^+$ and $CD11b^+/Ly6G^+$ progenitors that subsequently massively mobilized to tumors (Figs. 5, 6). These findings are consistent with widely reported PXL-dependent (6,32,44) increases in BM produced progenitors along with the evidence for their pro-metastatic effects upon arrival to primary (32) and distant tumor sites (44). However, this is the first evidence that both expansion of $CD11b^+/Ly6C^+/Ly6G^+$cells at TLR4-responsive organs and their recruitment to tumors is enhanced by taxane therapy and correlate with tumor-expressed TLR4. This notion is also consistent with reported mechanisms of creating pulmonary pre-metastatic niche through tumor-produced G-CSF and GM-CSF that mobilize $Ly6C^+/Ly6G^+$myeloid precursors from the BM to the lung (44). Noteworthy, PXL was reported to upregulate these factors by >20-fold in TLR4-positive BC lines (45). Collectively, these findings suggest that pro-metastatic effects of PXL•TLR4 axis are mediated, in part, by chemotherapy-induced factors in primary tumors that are released to systemic blood circulation and promote successful engraftment of malignant cells at secondary sites.

PXL therapy of TLR4$^+$ tumors creates intratumoral lymphatic vessels and promotes their invasion

One of the most remarkable and important findings in this study is the discovery that PXL therapy induced *de novo* formation of intratumoral lymphatics in TLR4$^+$ (but not negative) tumors (Fig. 7). It is currently believed that peritumoral lymphatic vessels are mainly responsible for malignant spread (31) because intratumoral lymphatics are rare in most untreated tumors including breast cancers that preferentially metastasize through these vessels (46). However, tumors that do generate intratumoral lymphatics are much more efficient in reaching LNs (47) resulting in a significantly higher risk for relapse and poorer prognosis (48). We show here that although blood and lymphatic vessels are both significantly increased in TLR4$^+$ tumors following chemotherapy, only the latter were invaded by tumor cells (Fig. 7). This suggests that the primary mechanism by which PXL•TLR4 axis promotes BC metastasis is through creation of penetration-permissive intratumoral channels that exponentially increase the number of malignant cells transported to the local nodes. This new mechanism in tumor biology might mirror a previously established ability of LPS-activated TLR4 pathway to promote lymphangiogenesis mediated by BM-derived macrophages recruited to the inflamed site (49). Analogously, the PXL•TLR4 pathway may induce intratumoral lymphangiogenesis mediated by CD11b$^+$ myeloid progenitors mobilized to the tumor site (Fig. 6). Thus, this discovery not only provides a likely explanation for PXL-mediated metastasis, but also suggests a novel way to study the formation of tumor lymphatics by comparing parallel steps of this monocyte-driven process induced by both chronic inflammation and cancer (50).

In summary, we show here that PXL chemotherapy substantially increases the magnitude of lymphatic and distant metastasis through activation of the TLR4 pathway in tumor cells which strongly elevates inflammation in the tumor environment, regional nodes, and distant organs thus favoring malignant outgrowth. The pro-metastatic phenotype is locally driven by *de novo* formation of intratumoral lymphatics and amplified systemically by expansion of myeloid pro-vascular progenitors and their recruitment to both primary and distant sites. Collectively, these findings suggest that blocking PXL-induced inflammation in patients with TLR4-positive cancers may significantly improve therapeutic outcome.

Supplementary Material

Refer to Web version on PubMed Central for supplementary material.

Acknowledgments

This work was supported by NIH grant 5R01CA140732 and by grants from the Illinois William E. McElroy Foundation awarded to Sophia Ran.

Abbreviations

BC	Breast cancer
BM	bone marrow

BVD	blood vessel density
CDS	complimentary DNA sequence
Cntrl	Control
DN	dominant-negative
LN(s)	lymph node(s)
LPS	lipopolysaccharide
LVD	lymphatic vessel density
MECA-32	anti-mouse pan endothelial cell antibody
MFP	mammary fat pad
nab-PXL	nab-paclitaxel
TLR4	Toll-like Receptor-4

References

1. Gradishar WJ, Tjulandin S, Davidson N, Shaw H, Desai N, et al. Phase III trial of nanoparticle albumin-bound paclitaxel compared with polyethylated castor oil-based paclitaxel in women with breast cancer. J Clin Oncol. 2005; 23:7794–7803. [PubMed: 16172456]
2. O'Shaughnessy J, Gradishar WJ, Bhar P, Iglesias J. Nab-paclitaxel for first-line treatment of patients with metastatic breast cancer and poor prognostic factors: a retrospective analysis. Breast Cancer Res Treat. 2013; 138:829–837. [PubMed: 23563958]
3. Kataja V, Castiglione M. Locally recurrent or metastatic breast cancer: ESMO clinical recommendations for diagnosis, treatment and follow-up. Ann Oncol. 2008; 19(Suppl 2):ii11–ii13. [PubMed: 18456744]
4. Gonzalez-Angulo AM, Morales-Vasquez F, Hortobagyi GN. Overview of resistance to systemic therapy in patients with breast cancer. Adv Exp Med Biol. 2007; 608:1–22. [PubMed: 17993229]
5. Szajnik M, Szczepanski MJ, Czystowska M, Elishaev E, Mandapathil M, et al. TLR4 signaling induced by lipopolysaccharide or paclitaxel regulates tumor survival and chemoresistance in ovarian cancer. Oncogene. 2009; 28:4353–4363. [PubMed: 19826413]
6. Daenen LG, Roodhart JM, van AM, Dehnad M, Roessingh W, et al. Chemotherapy enhances metastasis formation via VEGFR-1-expressing endothelial cells. Cancer Res. 2011; 71:6976–6985. [PubMed: 21975929]
7. Berrieman HK, Lind MJ, Cawkwell L. Do beta-tubulin mutations have a role in resistance to chemotherapy? Lancet Oncol. 2004; 5:158–164. [PubMed: 15003198]
8. Rajput S, Volk-Draper LD, Ran S. TLR4 is a novel determinant of the response to paclitaxel in breast cancer. Mol Cancer Ther. 2013; 12:1676–1687. [PubMed: 23720768]
9. Iwasaki A, Medzhitov R. Toll-like receptor control of the adaptive immune responses. Nat Immunol. 2004; 5:987–995. [PubMed: 15454922]
10. Mittal D, Saccheri F, Venereau E, Pusterla T, Bianchi ME, et al. TLR4-mediated skin carcinogenesis is dependent on immune and radioresistant cells. EMBO J. 2010; 29:2242–2252. [PubMed: 20526283]
11. Byrd-Leifer CA, Block EF, Takeda K, Akira S, Ding A. The role of MyD88 and TLR4 in the LPS-mimetic activity of Taxol. Eur J Immunol. 2001; 31:2448–2457. [PubMed: 11500829]
12. Hasimu A, Ge L, Li QZ, Zhang RP, Guo X. Expressions of Toll-like receptors 3, 4, 7, and 9 in cervical lesions and their correlation with HPV16 infection in Uighur women. Chin J Cancer. 2011; 30:344–350. [PubMed: 21527067]

13. Gonzalez-Reyes S, Fernandez JM, Gonzalez LO, Aguirre A, Suarez A, et al. Study of TLR3, TLR4, and TLR9 in prostate carcinomas and their association with biochemical recurrence. Cancer Immunol Immunother. 2010; 60:217–226. [PubMed: 20978888]

14. Gonzalez-Reyes S, Marin L, Gonzalez L, Gonzalez LO, Del Casar JM, et al. Study of TLR3, TLR4 and TLR9 in breast carcinomas and their association with metastasis. BMC Cancer. 2010; 10:665. [PubMed: 21129170]

15. Hsu RY, Chan CH, Spicer JD, Rousseau MC, Giannias B, et al. LPS-induced TLR4 signaling in human colorectal cancer cells increases beta1 integrin-mediated cell adhesion and liver metastasis. Cancer Res. 2011; 71:1989–1998. [PubMed: 21363926]

16. Zhang JJ, Wu HS, Wang L, Tian Y, Zhang JH, et al. Expression and significance of TLR4 and HIF-1alpha in pancreatic ductal adenocarcinoma. World J Gastroenterol. 2010; 16:2881–2888. [PubMed: 20556833]

17. Wang EL, Qian ZR, Nakasono M, Tanahashi T, Yoshimoto K, et al. High expression of Toll-like receptor 4/myeloid differentiation factor 88 signals correlates with poor prognosis in colorectal cancer. Br J Cancer. 2010; 102:908–915. [PubMed: 20145615]

18. Szczepanski MJ, Czystowska M, Szajnik M, Harasymczuk M, Boyiadzis M, et al. Triggering of Toll-like receptor 4 expressed on human head and neck squamous cell carcinoma promotes tumor development and protects the tumor from immune attack. Cancer Res. 2009; 69:3105–3113. [PubMed: 19318560]

19. Tang XY, Zhu YQ, Wei B, Wang H. Expression and functional research of TLR4 in human colon carcinoma. Am J Med Sci. 2010; 339:319–326. [PubMed: 20228668]

20. Ikebe M, Kitaura Y, Nakamura M, Tanaka H, Yamasaki A, et al. Lipopolysaccharide (LPS) increases the invasive ability of pancreatic cancer cells through the TLR4/MyD88 signaling pathway. J Surg Oncol. 2009; 100:725–731. [PubMed: 19722233]

21. Wang AC, Su QB, Wu FX, Zhang XL, Liu PS. Role of TLR4 for paclitaxel chemotherapy in human epithelial ovarian cancer cells. Eur J Clin Invest. 2009; 39:157–164. [PubMed: 19200169]

22. Zhu Y, Huang JM, Zhang GN, Zha X, Deng BF. Prognostic significance of MyD88 expression by human epithelial ovarian carcinoma cells. J Transl Med. 2012; 10:77. [PubMed: 22533866]

23. Kim KH, Jo MS, Suh DS, Yoon MS, Shin DH, et al. Expression and significance of the TLR4/MyD88 signaling pathway in ovarian epithelial cancers. World J Surg Oncol. 2012; 10:193. [PubMed: 22985132]

24. Earl TM, Nicoud IB, Pierce JM, Wright JP, Majoras NE, et al. Silencing of TLR4 decreases liver tumor burden in a murine model of colorectal metastasis and hepatic steatosis. Ann Surg Oncol. 2009; 16:1043–1050. [PubMed: 19165543]

25. van B Jr, Buurman WA, Griffioen AW. Convergence and amplification of toll-like receptor (TLR) and receptor for advanced glycation end products (RAGE) signaling pathways via high mobility group B1 (HMGB1). Angiogenesis. 2008; 11:91–99. [PubMed: 18264787]

26. Volk LD, Flister MJ, Chihade D, Desai N, Trieu V, et al. Synergy of nab-paclitaxel and bevacizumab in eradicating large orthotopic breast tumors and preexisting metastases. Neoplasia. 2011; 13:327–338. [PubMed: 21472137]

27. Li M, Carpio DF, Zheng Y, Bruzzo P, Singh V, et al. An essential role of the NF-kappa B/Toll-like receptor pathway in induction of inflammatory and tissue-repair gene expression by necrotic cells. J Immunol. 2001; 166:7128–7135. [PubMed: 11390458]

28. Mollen KP, Anand RJ, Tsung A, Prince JM, Levy RM, et al. Emerging paradigm: toll-like receptor 4-sentinel for the detection of tissue damage. Shock. 2006; 26:430–437. [PubMed: 17047512]

29. Peinado H, Rafii S, Lyden D. Inflammation joins the “niche”. Cancer Cell. 2008; 14:347–349. [PubMed: 18977322]

30. Movahedi K, Laoui D, Gysemans C, Baeten M, Stange G, et al. Different tumor microenvironments contain functionally distinct subsets of macrophages derived from Ly6C(high) monocytes. Cancer Res. 2010; 70:5728–5739. [PubMed: 20570887]

31. Volk-Draper LD, Rajput S, Hall KL, Wilber A, Ran S. Novel model for basaloid triple-negative breast cancer: behavior in vivo and response to therapy. Neoplasia. 2012; 14:926–942. [PubMed: 23097627]

32. DeNardo DG, Brennan DJ, Rexhepaj E, Ruffell B, Shiao SL, et al. Leukocyte complexity predicts breast cancer survival and functionally regulates response to chemotherapy. Cancer Discov. 2011; 1:54–67. [PubMed: 22039576]
33. Pusztai L, Mendoza TR, Reuben JM, Martinez MM, Willey JS, et al. Changes in plasma levels of inflammatory cytokines in response to paclitaxel chemotherapy. Cytokine. 2004; 25:94–102. [PubMed: 14698135]
34. Altorki NK, Port JL, Zhang F, Golijanin D, Thaler HT, et al. Chemotherapy induces the expression of cyclooxygenase-2 in non-small cell lung cancer. Clin Cancer Res. 2005; 11:4191–4197. [PubMed: 15930356]
35. Silasi DA, Alvero AB, Illuzzi J, Kelly M, Chen R, et al. MyD88 predicts chemoresistance to paclitaxel in epithelial ovarian cancer. Yale J Biol Med. 2006; 79:153–163. [PubMed: 17940625]
36. Kajiyama H, Shibata K, Terauchi M, Yamashita M, Ino K, et al. Chemoresistance to paclitaxel induces epithelial-mesenchymal transition and enhances metastatic potential for epithelial ovarian carcinoma cells. Int J Oncol. 2007; 31:277–283. [PubMed: 17611683]
37. Aggarwal BB, Shishodia S, Takada Y, Banerjee S, Newman RA, et al. Curcumin suppresses the paclitaxel-induced nuclear factor-kappaB pathway in breast cancer cells and inhibits lung metastasis of human breast cancer in nude mice. Clin Cancer Res. 2005; 11:7490–7498. [PubMed: 16243823]
38. Voelcker V, Gebhardt C, Averbeck M, Saalbach A, Wolf V, et al. Hyaluronan fragments induce cytokine and metalloprotease upregulation in human melanoma cells in part by signalling via TLR4. Exp Dermatol. 2008; 17:100–107. [PubMed: 18031543]
39. Schelbergen RF, Blom AB, van den Bosch MH, Sloetjes A, Abdollahi-Roodsaz S, et al. Alarmins S100A8 and S100A9 elicit a catabolic effect in human osteoarthritic chondrocytes that is dependent on Toll-like receptor 4. Arthritis Rheum. 2012; 64:1477–1487. [PubMed: 22127564]
40. Kim S, Takahashi H, Lin WW, Descargues P, Grivennikov S, et al. Carcinoma-produced factors activate myeloid cells through TLR2 to stimulate metastasis. Nature. 2009; 457:102–106. [PubMed: 19122641]
41. Zheng H, Heiderscheidt CA, Joo M, Gao X, Knezevic N, et al. MYD88-dependent and -independent activation of TREM-1 via specific TLR ligands. Eur J Immunol. 2010; 40:162–171. [PubMed: 19904768]
42. Diaz-Montero CM, Salem ML, Nishimura MI, Garrett-Mayer E, Cole DJ, et al. Increased circulating myeloid-derived suppressor cells correlate with clinical cancer stage, metastatic tumor burden, and doxorubicin-cyclophosphamide chemotherapy. Cancer Immunol Immunother. 2009; 58:49–59. [PubMed: 18446337]
43. El Sharouni SY, Kal HB, Battermann JJ. Accelerated regrowth of non-small-cell lung tumours after induction chemotherapy. Br J Cancer. 2003; 89:2184–2189. [PubMed: 14676792]
44. Kowanetz M, Wu X, Lee J, Tan M, Hagenbeek T, et al. Granulocyte-colony stimulating factor promotes lung metastasis through mobilization of Ly6G+Ly6C+ granulocytes. Proc Natl Acad Sci USA. 2010; 107:21248–21255. [PubMed: 21081700]
45. Zaks-Zilberman M, Zaks TZ, Vogel SN. Induction of proinflammatory and chemokine genes by lipopolysaccharide and paclitaxel (Taxol) in murine and human breast cancer cell lines. Cytokine. 2001; 15:156–165. [PubMed: 11554785]
46. Ran S, Volk L, Hall K, Flister MJ. Lymphangiogenesis and lymphatic metastasis in breast cancer. Pathophysiology. 2009; 17:229–251. [PubMed: 20036110]
47. Beasley NJ, Prevo R, Banerji S, Leek RD, Moore J, et al. Intratumoral lymphangiogenesis and lymph node metastasis in head and neck cancer. Cancer Res. 2002; 62:1315–1320. [PubMed: 11888898]
48. Maula SM, Luukkaa M, Grenman R, Jackson D, Jalkanen S, et al. Intratumoral lymphatics are essential for the metastatic spread and prognosis in squamous cell carcinomas of the head and neck region. Cancer Res. 2003; 63:1920–1926. [PubMed: 12702584]
49. Kang S, Lee SP, Kim KE, Kim HZ, Memet S, et al. Toll-like receptor 4 in lymphatic endothelial cells contributes to LPS-induced lymphangiogenesis by chemotactic recruitment of macrophages. Blood. 2009; 113:2605–2613. [PubMed: 19098273]

50. Ran S, Montgomery KE. Macrophage-mediated lymphangiogenesis: the emerging role of macrophages as lymphatic endothelial progenitors. Cancers. 2012; 4:618–657. [PubMed: 22946011]

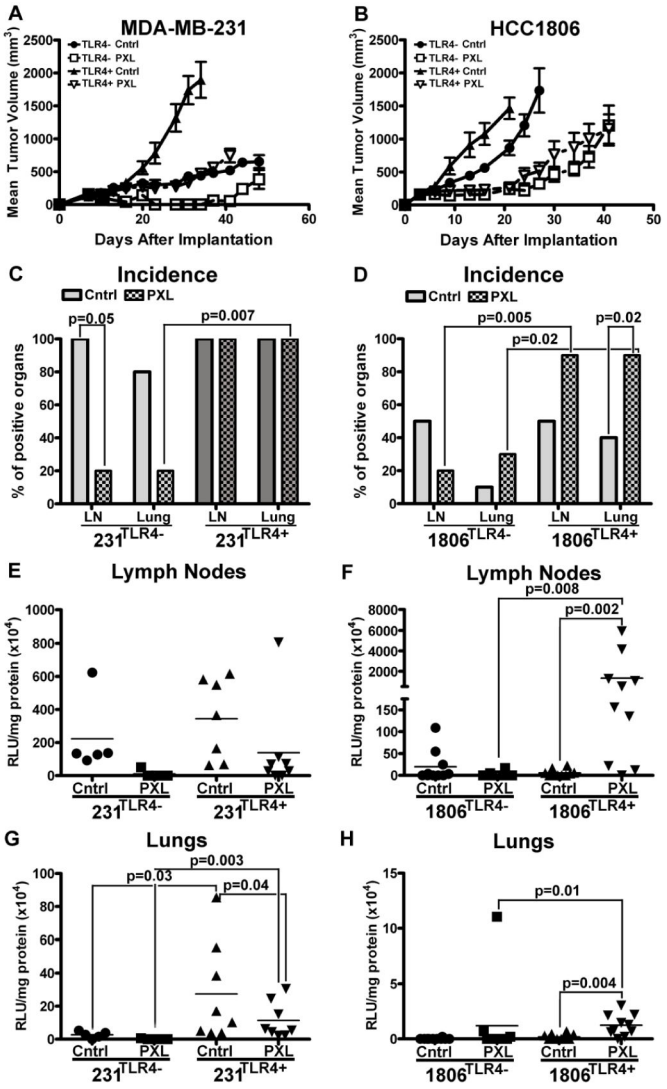

Figure 1. The effects of nab-PXL treatment on MDA-MB-231 and HCC1806 tumors with modified TLR4 expression in vivo

MDA-MB-231 and HCC1806 were genetically engineered, respectively, to suppress or overexpress TLR4. Lines with modified TLR4 expression were designated as $231^{TLR4-}$and 1806^{TLR4+}whereas corresponding controls were labeled as 231^{TLR4+} and 1806^{TLR4-}. Growth of orthotopically implanted (A) MDA-MB-231 and (B) HCC1806 is presented as the mean tumor burden ± SEM. Untreated controls are denoted with "Cntrl" and treatment with nab-PXL indicated by "PXL". Incidence of metastasis to the lymph nodes (LNs) and lungs was assessed for (C) MDA-MB-231 and (D) HCC1806 cell lines. Each bar represents the percentage of mice with positive organs as assessed by luciferase assay. Statistical analysis was performed by a Fisher Exact test. The metastatic burden of lymph nodes (E & F) and lungs (G & H) was assessed in MDA-MB-231 (E & G) and HCC1806 (F & H). Each dot represents an individual mouse's metastatic burden in RLU/mg protein $x10^4$. Statistical analysis for differences in metastatic burden was performed by Mann-Whitney test. The black bars indicate the mean metastatic burden in each group (n=5–10). Black brackets

indicate statistical significance between groups with corresponding P-value listed above the bracket.

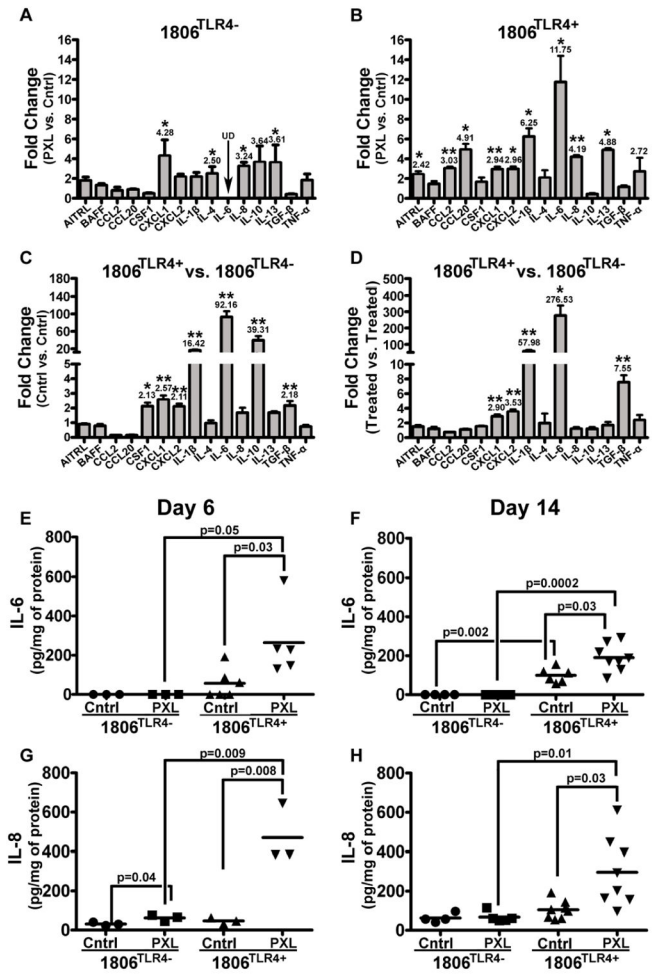

Figure 2. Treatment with nab-PXL increases inflammatory cytokine expression in the local tumor environment

Mice with 1806^{TLR4-} and 1806^{TLR4+} tumors were treated with nab-PXL (10mg/kg) for five days. Message RNA extracted from untreated (Cntrl) and treated (PXL) tumors on the day following the last day of treatment was analyzed by RT-qPCR. Changes in transcript expression of human inflammatory cytokines were compared between nab-PXL treated vs. Cntrl tumors in mice bearing 1806^{TLR4-} (A) and 1806^{TLR4+} (B). Similar analysis was performed comparing 1806^{TLR4+} and 1806^{TLR4-} tumors in untreated (C) and nab-PXL-treated (D) mice. Graphs show changes in cytokines that increased more than 2 fold. Black arrows labeled with UD indicate undetectable transcript levels. Asterisks * and ** indicate P-values of <0.05 and ≤0.01, respectively, as determined by Student's t-test. Human IL-6 (E & F) and IL-8 (G & H) proteins levels were measured in tumor lysates by ELISA from mice on the 6^{th} (E & G) and 14^{th} (F & H) day of treatment. The results are expressed as pg/mg of protein. Each dot represents an individual mouse's protein expression and the black bar indicates the mean cytokine expression per group. Black brackets indicate statistical significance between groups with the corresponding P-value determined by a Student's t-test. Each ELISA was performed in duplicate and reproduced twice.

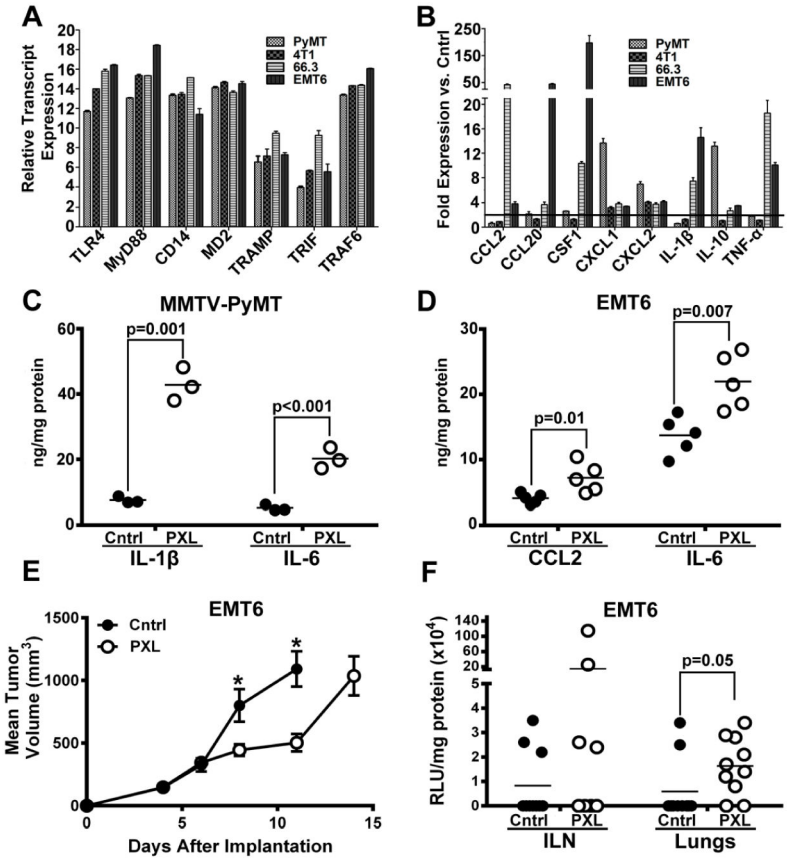

Figure 3. Syngeneic BC mouse models overexpress TLR4 and react to nab-PXL by increasing inflammatory cytokines and metastatic spread

Four mouse BC cell lines (MMTV-PyMT, 4T1, 66.3 and EMT6) were analyzed by RT-qPCR for expression of TLR4 and main components of the TLR4 pathway (A). Cell lines were treated with 30 nM of nab-PXL followed by RT-qPCR analysis of a panel of mouse inflammatory cytokines typically upregulated in human tumor cells (B). Female BALB/c or C57BL/6 mice were orthotopically implanted with 0.5×10^6 of MMTV-PyMT or EMT6 cells. When tumors reached 200 mm^3, mice were treated with nab-PXL (30 mg/kg) for 5 days. Tumors were extracted on day 6 post-treatment and analyzed for expressions of inflammatory cytokines by ELISA. The most upregulated cytokines in MMTV-PyMT (C) and EMT6 (D) models are shown. ELISA analysis was performed in duplicate and repeated twice. The data are expressed in ng normalized per mg of total protein and each circle represents the average value for an individual mouse. The black bars indicate the mean cytokine concentration in each group (n=10). Black brackets indicate statistical significance between groups with corresponding P-value listed above the bracket. (E) The mean volumes of EMT6-luciferase tagged tumors in control (untreated) and nab-PXL treated group (n=10). Asterisks indicate statistically significant differences between the mean volumes in control and treated groups. (F) Luciferase activity normalized per mg of total protein was measured in ipsilateral LNs and lungs in control and nab-PXL groups (n=10). Results are presented as RLU/mg protein detected in individual mice. The black bars show the mean value per group

and the black bracket with the corresponding P-value determined by a Student's t-test shows significance between tested groups.

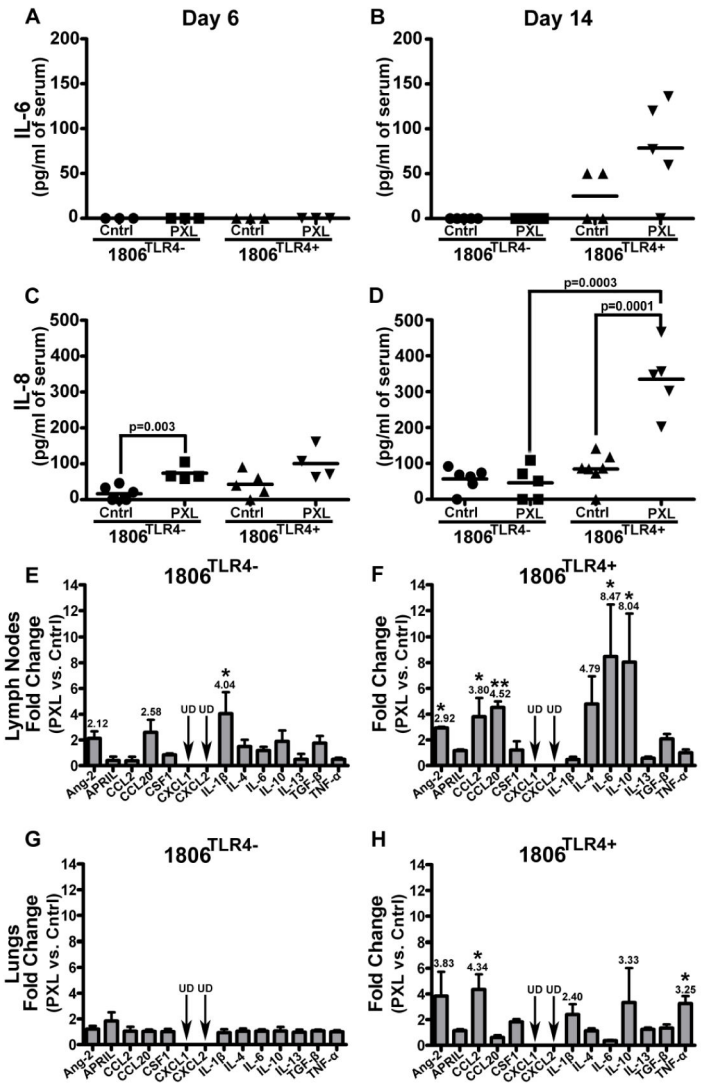

Figure 4. Treatment with nab-PXL systemically increases inflammatory cytokine expression in circulation and distant organs in vivo

1806^{TLR4-} and 1806^{TLR4+} tumors were treated for five days with nab-PXL followed by harvesting LN, lungs and serum on the 6th and 14th day of treatment. Serum levels of human IL-6 (A & B) and IL-8 (C & D) proteins were measured by ELISA. The results expressed as pg/ml of serum show cytokine expression on the 6th (A & C) and 14th (B & D) day post-treatment. Each dot represents an individual mouse's protein expression and the black bar indicates the mean cytokine concentration per group. Black brackets indicate statistical significance between two groups with the corresponding P-value determined by a Student's t-test. Each ELISA was performed twice in duplicate. Panels E to H show changes in mRNA expression of human cytokines on the 14th day post-treatment in lymph nodes (E & F) and lungs (G & H) determined by RT-qPCR. E and G panels show changes in the lymph nodes and lungs of nab-PXL (PXL) treated as compared to untreated mice bearing TLR4-negative tumors (Cntrl). F and H show changes in treated and untreated mice bearing TLR4-positive tumors. Cytokines that increased more than 2-fold are shown. Black arrows labeled by UD

indicate undetectable transcript levels. Asterisks * and ** indicate P-values of <0.05 and ≤0.01, respectively, as determined by Student's t-test.

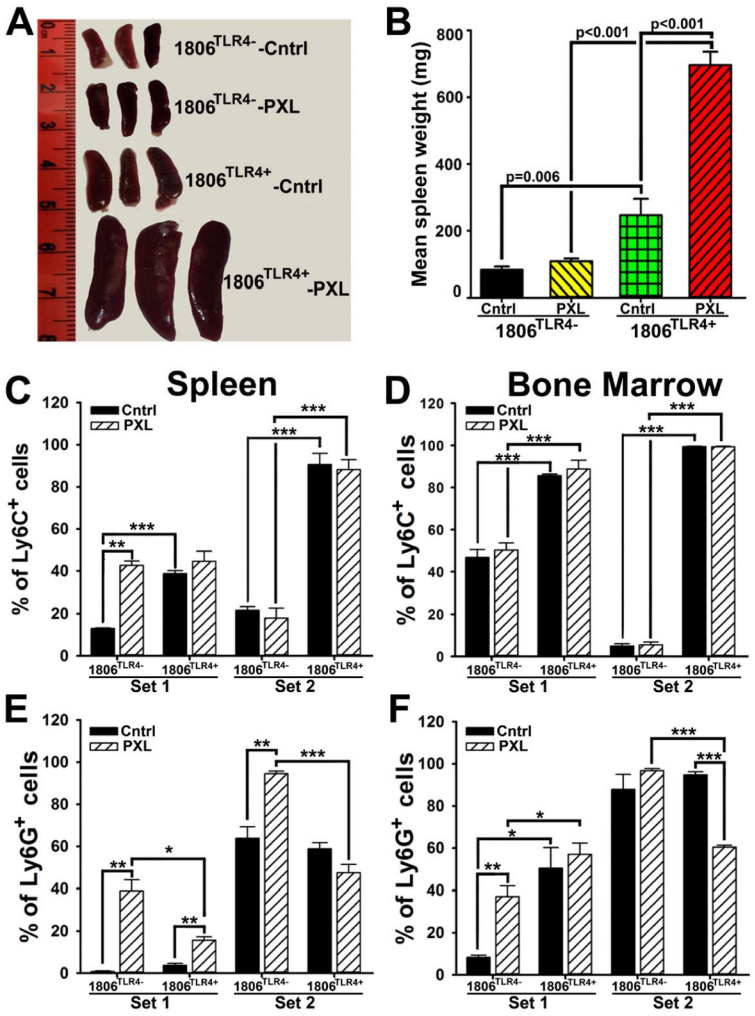

Figure 5. TLR4 overexpression and nab-PXL treatment increase generation of myeloid progenitor cells in distant organs

(A) Imaged spleens from untreated (Cntrl) and nab-PXL (PXL) treated mice bearing 1806^{TLR4-} and 1806^{TLR4+} tumors. (B) Spleen weight is presented as the mean mg ± SEM. Panels C–F show FACS analysis of $CD11b^+$ myeloid progenitors isolated from spleens (C & E) and BM (D & F). The spleen and BM fractions of $CD11b^+/Ly6C^+$ or $CD11b^+/Ly6G^+$ are shown in panels C & E and D & F, respectively. The data are presented as the mean percentage of double-positive cells ± SEM per group of 3 to 5 mice. Cell populations comprising Set 1 and Set 2 are defined in supplementary Fig. S3. Black brackets indicate statistical significance with corresponding P-value listed above or noted by asterisks *, **, and *** (P-values of <0.05, <0.01, and <0.001, respectively), as determined by a Student's t-test.

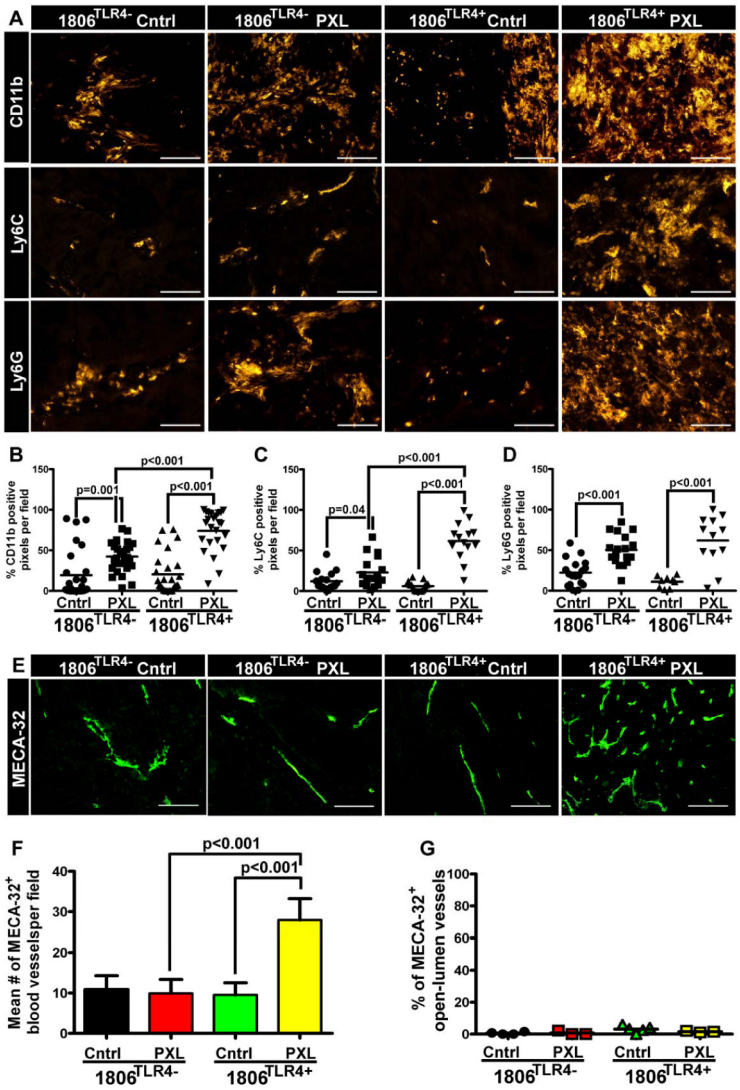

Figure 6. TLR4 expression and nab-PXL treatment promote myeloid cell recruitment and tumor blood vasculature

Sections of 1806^{TLR4-} and 1806^{TLR4+} tumors from control mice and treated with nab-PXL (10 mg/kg, 5 days) were stained for myeloid markers CD11b, Ly6C, and Ly6G (A). The extent of myeloid cell recruitment was quantified by measuring the pixel intensity from positive immunoreaction on 6–10 fields per slide for CD11b (B), Ly6C (C), and Ly6G (D). Each dot represents values of positive pixels determined on individual slides and the black bar indicates the mean percentage of positive pixels. Blood vessel density (BVD) was determined in tumors collected on the 21st day post-treatment using antibody against MECA-32 (E). Changes in BVD were determined as described under Methods and normalized per field. (F). Blood vessel invasion was determined as described under Methods in an entire tumor cross-section. The results are presented as the percent of tumor invaded vessels from total open-lumen blood vessels identified by MECA-32 (G). In all graphs, the black brackets indicate statistical significance with corresponding P-value listed above by a Student's t-test. All images were acquired at 200X magnification and scale bars are 100μm.

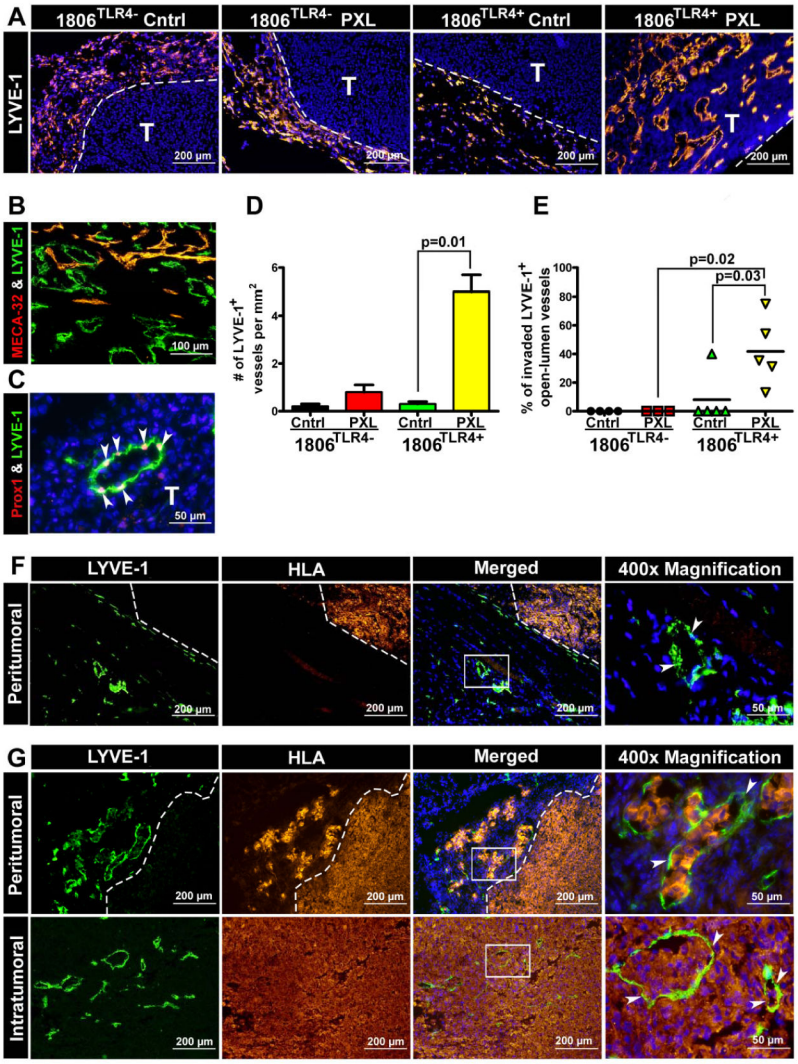

Figure 7. Nab-PXL treatment of TLR4^{+} tumors induces intratumoral lymphatic vessels and promotes their invasion

Sections of 1806^{TLR4-} and 1806^{TLR4+} tumors from mice treated with nab-PXL (10 mg/kg, 5 days) were stained for Lyve-1 (A). All images were taken at magnification of 100x. Tumor sections were co-stained with (B) Lyve-1 & MECA-32 (200x), and (C) Lyve-1 & Prox1 (400x) to verify lymphatic identity. White arrowheads point to Prox1 positive nuclei embedded in the luminal Lyve-1 positive lymphatic vessel. (D) Lymphatic vessel density (LVD) was calculated as described in Methods and normalized by area. LVD is presented as the mean number of Lyve-1^{+} vessels per mm^{2}. (E, F) Lymphatic vessel invasion (LVI) was determined by co-staining with anti-Lyve-1 and anti-HLA antibodies as described in the Methods. (E) Quantification of LVI in TLR4-positive and TLR4-negative tumors that were either treated with nab-PXL or untreated. Each dot represents the percent of invaded open-lumens per tumor. (F) Representative images of uninvaded peritumoral lymphatic vessels by human HLA^{+} tumors cells from 1806^{TLR4+} untreated tumors. (G) Representative images of invaded peritumoral and intratumoral lymphatic vessels by human HLA^{+} tumor cells derived from 1806^{TLR4+} treated tumors. All images were acquired at magnification of 100x

except the far right image marked by “400x Magnification.” White boxes indicate the magnified region of the image and white arrowheads point to the highlighted open-lumen vessel. In all images white dashed-lines mark the tumor-host border. White letter “T” indicates tumor tissue. In graphs, the black brackets indicate statistical significance with corresponding P-value listed above as determined by a Student’s t-test.